JOC The Journal of Organic Chemistry

ARTICLE

pubs.acs.org/joc

Oxidation of Annelated Diarylamines: Analysis of Reaction Pathways to Nitroxide Diradical and Spirocyclic Products

Andrzej Rajca,*[,†] Kouichi Shiraishi,[†] Przemysław J. Boratyński,[†,§] Maren Pink,[‡] Makoto Miyasaka,[†] and Suchada Rajca[†]

[†]Department of Chemistry, University of Nebraska, Lincoln, Nebraska 68588-0304, United States

[‡]IUMSC, Department of Chemistry, Indiana University, Bloomington, Indiana 47405-7102, United States

Supporting Information

ABSTRACT: Oxidation of diaryldiamine **2**, a tetrahydrodiazapentacene derivative, provides diarylnitroxide diradical **1** accompanied by an intermediate nitroxide monoradical and a multitude of isolable diamagnetic products. DFT-computed tensors for EPR spectra and paramagnetic ^{1}H NMR isotropic shifts for nitroxide diradical **1** show good agreement with the experimental EPR spectra in rigid matrices and paramagnetic ^{1}H NMR spectra in solution, respectively. Examination of the diamagnetic products elucidates their formation via distinct pathways involving C−O bond-forming reactions, including Baeyer−Villiger-type oxidations. An unusual diiminoketone structure and two spirocyclic structures of the predominant diamagnetic products are confirmed by either X-ray crystallography or correlations between DFT-computed and experimental spectroscopic data such as ^{1}H, ^{13}C, and ^{15}N NMR chemical shifts and electronic absorption spectra.

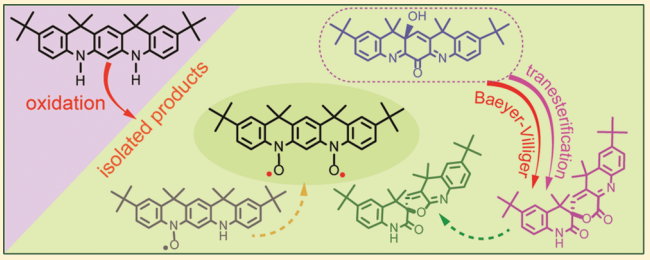

INTRODUCTION

Stable nitroxides are an important class of free radicals with a wide range of applications in organic synthesis, biophysics, biomedicine, and materials chemistry.[1−9] Such stable radicals are typically prepared by oxidation of secondary amines with peroxy-based reagents. For example, oxidation of sterically hindered secondary dialkylamines with *m*-chloroperbenzoic acid (*m*-CPBA) or dimethyldioxirane (DMDO) provides the corresponding nitroxides in high yields.[10,11] However, these peroxy-based reagents are considerably less efficient for oxidation of secondary arylamines, and especially diarylamines, to provide the corresponding arylnitroxides and diarylnitroxides.[12,13] This difficulty contributes to the scarcity of diarylnitroxides.[14−18]

We recently reported the isolation of a stable diarylnitroxide diradical **1** with triplet ground state and singlet−triplet energy gap (ΔE_{ST}) exceeding thermal energy at room temperature (0.6 kcal mol^{-1}).[19] Because at room temperature the triplet ground state is significantly populated[19,20] and its diarylnitroxide moieties allow for a direct extension of the π-system to provide for effective contacts, the structural motif of **1** is promising for spintronics applications.[21] In addition, diarylnitroxide radicals with alternating connectivity of nitroxide radicals and *m*-phenylene ferromagnetic coupling units are attractive building blocks for high-spin polyradicals that could be useful in the development of organic magnetic materials.[22−25]

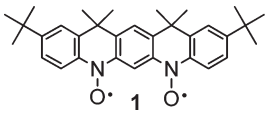

In the synthesis of **1**, we found that oxidations of secondary diaryl diamines to form the corresponding diaryl nitroxides using peroxy-based reagents are problematic. When dibenzoyl peroxide (BPO) was used as an oxidant, the annelated diamine **2** splendidly underwent three oxidative CC and NN couplings to give the conjoined double [5]helicene and nitroxide diradical **1** was not detected.[26] Oxidation of **2** with DMDO in dichloromethane (DCM) at low temperatures (−78 to −40 °C)[14] provided reaction mixtures in which nitroxide diradical **1** was detected at low temperatures by EPR spectroscopy.[19] Oxidation of **2** with *m*-CPBA in DCM at 0 °C gave nitroxide diradical **1** in about 20% isolated yields.[19]

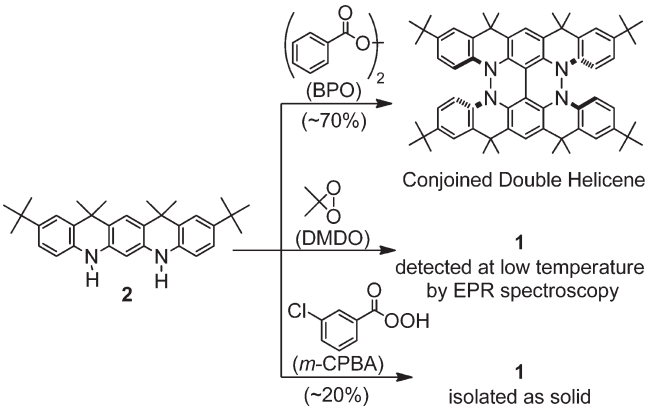

Received: August 30, 2011
Published: September 06, 2011

dx.doi.org/10.1021/jo2017923 | J. Org. Chem. 2011, 76, 8447–8457

Scheme 1. Reaction of Diamine 2 with 6 equiv of *m*-CPBA

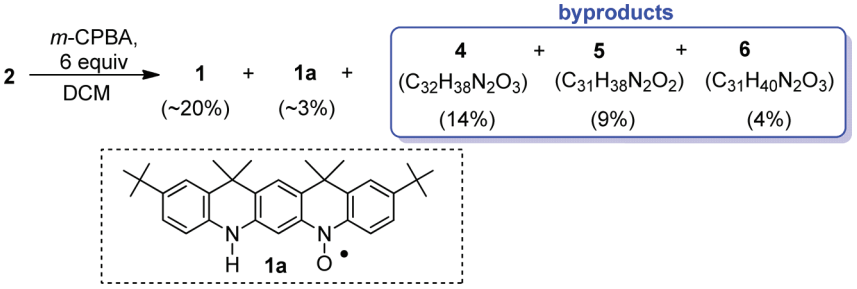

These intriguing results prompted us to investigate the oxidation reactions of diaryldiamine **2**. In addition to diradical **1**, we isolated monoradical and diamagnetic products from reaction of **2** with DMDO and *m*-CPBA. We also obtained the DFT-computed EPR spectra for diradical **1** and paramagnetic ^{1}H NMR spectra for diradical **1** and its monoradical precursor. These investigations provide a wealth of information on the oxidation of diaryldiamine **2**, for which we report herein the analysis of reaction pathways to diradical **1**, an unusual diiminoketone structure, and two spirocyclic structures of diamagnetic products.

RESULTS AND DISCUSSION

Oxidation of Diamine 2 with DMDO. Oxidation of diamine **2** with DMDO (~4−8 equiv) is carried out at −78 to −20 °C in acetone or DCM under conditions similar to those previously described.[14,19] After workup at ambient temperature, ^{1}H NMR spectra of the crude reaction mixtures show one predominant diamagnetic product (Figure S31, Supporting Information). However, the isolated yield of this product is only ~40%. The FABMS, employing a matrix containing sodium salts, shows the peak corresponding to $[M + Na]^+$ ion with dominant intensity in the m/z 350−1000 range, and its mass is within <3.4 ppm of the calculated value for $C_{32}H_{38}N_2O_2Na_1$, indicating that this product is a diamagnetic isomer of nitroxide diradical **1** ($C_{32}H_{38}N_2O_2$). We assign this product as structure **3** (eq 1), though other alternative structures may not be excluded.

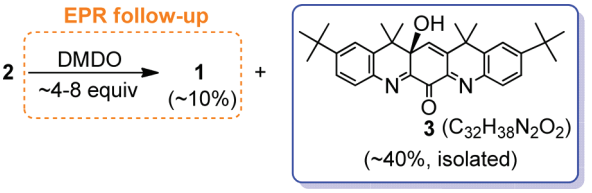

(1)

Oxidation of Diamine 2 with *m*-CPBA. Oxidation of diamine **2** with *m*-CPBA is carried out at 0 °C in DCM, for which we explored the reactions using 6, 4, and 2 equiv of *m*-CPBA.

We recently reported isolation of nitroxide diradical **1** in ~20% yield from reactions of diamine **2** with 6 equiv of *m*-CPBA in DCM, followed by a rapid filtration through deactivated silica gel.[19] Although EPR spectra of the isolated nitroxide diradical in frozen solution showed only a small content of monoradical byproduct, paramagnetic susceptibility studies by superconducting quantum interference device (SQUID) magnetometry in the solid state, as well as the NMR-based Evans method in solution, indicated significant content of diamagnetic byproducts. Thorough purification of the products from similar oxidations give diradical **1** in 5−10% isolated yields, for which a negligible content of paramagnetic and diamagnetic byproducts was detected, as determined by EPR spectroscopic and magnetic data.[19]

Scheme 2. Crude Reaction Mixtures from Reaction of Diamine 2 with *m*-CPBA According to ^{1}H NMR and LR-FABMS Analysis

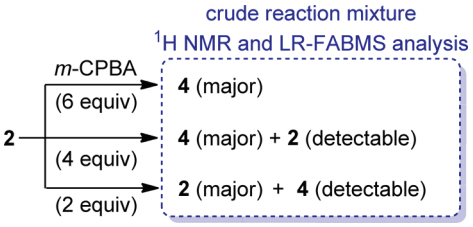

In these crude reaction mixtures, we now identify nitroxide monoradical **1a**, as well as three diamagnetic byproducts, **4** ($C_{32}H_{38}N_2O_3$), **5** ($C_{31}H_{38}N_2O_2$), and **6** ($C_{31}H_{40}N_2O_3$), which are isolated in 14%, 9%, and 4% yields, respectively (Scheme 1). ^{1}H NMR spectra of the reaction mixtures show **4** as the dominant component; in the mass spectra, the relative intensities for the ions corresponding to **4**, **5**, and **6** depend on the ionization method (EI vs FAB) and the matrix in FAB (Scheme 2) (Table S12, Supporting Information). Notably, structure of the dominant byproduct **4** has one more oxygen atom than **3**.

We further investigated the oxidation of diamine **2** using 4 and 2 equiv of *m*-CPBA in DCM by ^{1}H NMR spectroscopy and mass spectrometry (LR-FABMS). The reaction using 4 equiv of *m*-CPBA gives a crude reaction mixture that contains mostly byproduct **4**, as confirmed by the $[M + H]^+$ at m/z 499.3, with an admixture of the starting diamine **2**. When the oxidation of **2** is carried out using 2 equiv of *m*-CPBA, the crude reaction mixtures show predominantly the starting diamine **2** (FABMS: $[M]^+$ at m/z 453.3 and $[M - CH_3]^+$ at m/z 437.3) and a lower content of **4** (Supporting Information). Similar results are obtained for oxidation of diamine **2** using 6, 4, and 2 equiv of *m*-CPBA in benzene at 6 °C (Scheme 2).

Separation of crude reaction mixtures obtained using 2 equiv of *m*-CPBA produces unreacted diamine **2** in about 40% yield. Monoradical **1a** and byproduct **4** are isolated in low yields, as well as trace amounts of byproducts **5** and **6** (eq 2).

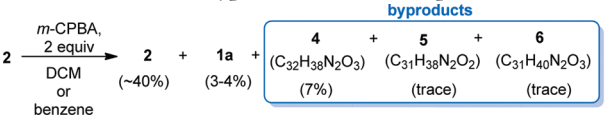

(2)

dx.doi.org/10.1021/jo2017923 |J. Org. Chem. 2011, 76, 8447–8457

Scheme 3. Oxidations of Diamine 2 with Na_2WO_4/H_2O_2 and *m*-CPBA

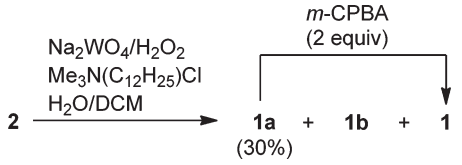

Oxidation of Diamine 2 with Other Oxidants. We also explored oxidation of diamine **2** with other common oxidants. Reactions of **2** with 4-methoxyperbenzoic acid lead primarily to diamagnetic byproducts.[27] However, the reaction of **2** using Na_2WO_4/H_2O_2 under phase-transfer catalysis leads to the formation of nitroxide monoradical **1a** (with a small admixture of diradical **1**) that is isolated in ~30% yield (Scheme 3). In addition, another paramagnetic product **1b** with complex hyperfine splittings in the EPR spectra is isolated (Figure S30, Supporting Information).

Upon further oxidation with *m*-CPBA, monoradical **1a** gives nitroxide diradical **1** (Figures S28 and S29, Supporting Information), though the overall isolated yields, based upon diamine **2**, are low. Thus, nitroxide monoradical **1a** is likely an intermediate in oxidation of diamine **2** with *m*-CPBA (6 equiv) to nitroxide diradical **1**.

Analysis of the Isolated Paramagnetic Products: Diradical 1 and Monoradical 1a. Although **1** was isolated as a solid, attempts to grow adequate crystals for an X-ray structure determination were not successful. Therefore, we relied on the correlation between the experimental and DFT-computed EPR spectra for the structural analysis for **1**, as well as for the intermediate monoradical **1a**. Analogous analyses have routinely been applied to NMR and electronic spectra of moderate-size organic molecules,[28−30] and recent advances in DFT methods make such computations feasible for organic monoradicals and diradicals, i.e., EPR spectra in glassy solutions and paramagnetic ^{1}H NMR spectra in fluid solutions.[31−35]

The geometries of **1** and **1a** are optimized at the UB3LYP/6-31G(d,p)+ZPVE level.[36] In both **1** and **1a**, the π-system composed of benzene rings and nitroxides is planar, similar to that in the X-ray structure of diamine **2**.[26] Anisotropic *D*-, *g*- and *A*-tensors are computed at the UB3LYP/EPR-II level using ORCA[37] for EPR spectra in rigid matrices (glassy solutions). Isotropic electron−nucleus hyperfine coupling constants (or splittings $a_{iso}/2$ for triplet diradical and a_{iso} for doublet monoradical) are calculated at the UB3LYP/EPR-III levels using Gaussian 09[36] for EPR spectra and paramagnetic ^{1}H NMR spectra in fluid solutions.

EPR Spectra for ***1***. Experimental EPR spectrum for diradical **1** in glassy toluene at 140 K shows six symmetrically positioned side bands that are associated with a triplet state with moderate values of zero-field splitting (zfs) parameters, *D* and *E*. The DFT calculation, based upon spin−spin only approximation (magnetic dipole−dipole interaction between unpaired electrons), somewhat overestimates the spacing of the outer Z-bands, $2|D|$, and the spacings of the inner X- and Y-bands, approximately $3|E|$ (Figure 1).[31,34] ^{14}N hyperfine coupling of two nitrogens splits the inner Y-bands into quintets as expected for the planar nitroxide-*m*-phenylene-nitroxide π-system in **1**. The spacings within the quintet should correspond to $|A_{YY}|/2$, where A_{YY} is the largest principal value of the ^{14}N *A*-tensor oriented parallel to the direction of the $2p_\pi$ orbital on the nitrogens

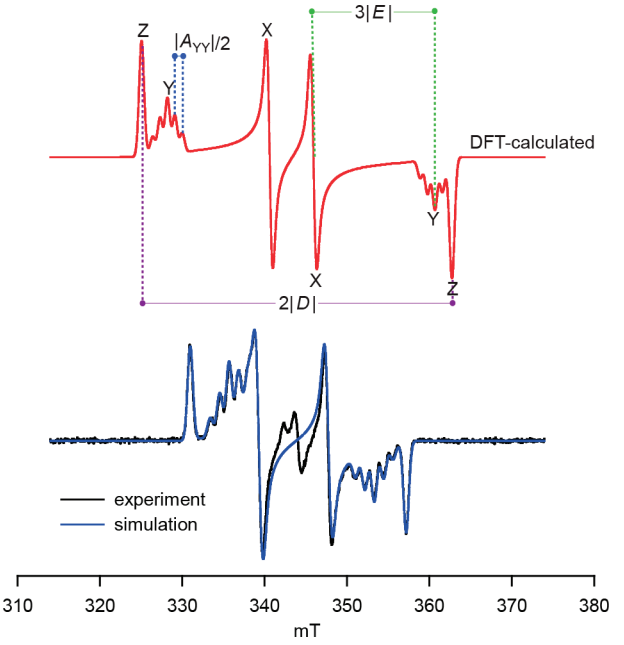

Figure 1. EPR spectra for nitroxide diradical **1**. Top: DFT-calculated spectrum at the UB3LYP/EPR-II level of theory. Bottom: experimental spectrum in toluene at 140 K and spectral simulation. Tensors obtained from spectral simulation of the experimental spectrum and from DFT calculations are summarized in Table 1.

(*Y*-axis). The DFT-calculated values of $A_{YY}/2 = 0.837 \times 10^{-3}$ cm^{-1} and 0.892×10^{-3} cm^{-1} at the UB3LYP/EPR-II and UB3LYP/EPR-III levels, respectively, slightly underestimate the experimental value of 1.06×10^{-3} cm^{-1}. The positions of each pair of the bands, labeled by X, Y, and Z in Figure 1, is determined by the corresponding principal values of the *g*-tensor, that is, g_{XX}, g_{YY}, g_{ZZ}. The DFT-calculated values of g_{XX}, g_{YY}, g_{ZZ}, using coupled-perturbed Kohn−Sham (CP-KS) theory at the UB3LYP/EPR-II level,[32] are in good agreement with the corresponding experimental values, including the isotropic *g*-value, $g_{iso} = (g_{XX} + g_{YY} + g_{ZZ})/3$ (Table 1).

EPR Spectra for ***1a***. The EPR spectrum of nitroxide monoradical **1a** in toluene at room temperature can be adequately simulated with a simple set of ^{14}N and ^{1}H hyperfine splittings (Figure 2 and Figure S28, Supporting Information). For **1a** in toluene, the ^{14}N hyperfine splitting is greater and the ^{1}H hyperfine splitting at the *ortho*-positions is smaller than analogous values of 0.97 and 0.19 mT in 4,4-di-*tert*-butyl-diphenylnitroxide radical in toluene,[14] as expected for greater delocalization of spin density from nitroxide to the phenyls in the planar structure of **1a**. DFT-calculated hyperfine splittings at the UB3LYP/EPR-III level of theory reproduce the experimental values qualitatively (Figure 2). The calculated $g_{iso} = 2.0053$ at the UB3LYP/EPR-II level (CP-KS theory) is also in good agreement with the experimental value of $g_{iso} = 2.0051$ in toluene at room temperature.

^{1}H NMR Spectra for ***1*** *and* ***1a***. Paramagnetic ^{1}H NMR spectra provide structural information that is complementary to the EPR spectra. ^{1}H NMR spectra of concentrated, fluid solutions of organic radicals (~0.1 M and higher) typically could be obtained for those protons with relatively low spin densities,[13,33,35,38] which usually possess too small hyperfine splittings to be resolved in the EPR spectra. Because the paramagnetic shifts in

dx.doi.org/10.1021/jo2017923 |J. Org. Chem. 2011, 76, 8447–8457

Table 1. Selected EPR and ^{1}H NMR Spectral Parameters for Nitroxide Diradical 1 Calculated at the UB3LYP/EPR-II and UB3LYP/EPR-III Levels of Theory[a]

	$D \times 10^3$ (cm^{-1})	$E \times 10^3$ (cm^{-1})	$^{14}N\ A_{YY}/2 \times 10^3$ (cm^{-1})	$^{14}N\ A_{iso}/2 \times 10^3$ (cm^{-1})	g_{XX}	g_{YY}	g_{ZZ}	g_{iso}	^{1}H (*t*-Bu) δ (ppm)	^{1}H (CMe_2) δ (ppm)
EPR-II	−17.7	−4.22	0.837	0.258	2.0083	2.0022	2.0055	2.0053		
EPR-III			0.892	0.272					9.0[b]	12.8[b]
experiment[c]	12.25	1.40	1.06		2.0076	2.0020	2.0047	2.0045	9.0	9.0

[a] UB3LYP/EPR-II and UB3LYP/EPR-III using ORCA and Gaussian09, respectively; optimized geometries at the UB3LYP/6-31G(d,p)+ZPVE level using Gaussian09. [b] Chemical shifts calculated using averaged isotropic ^{1}H hyperfine couplings for two C_{2v}-symmetric conformations of **1**, corresponding to 180° rotation of the *tert*-butyl groups (Tables S1 and S2, Supporting Information). [c] EPR spectrum in toluene at 140 K and ^{1}H NMR spectrum in chloroform-*d* at room temperature; signs of the zero-field splitting parameters *D* and *E* not determined by the experiment.[19]

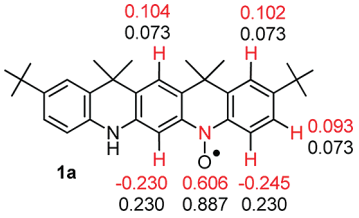

Figure 2. Structure for the nitroxide monoradical **1a**, illustrating UB3LYP/EPR-III-computed (red) and experimental (black) ^{1}H and ^{14}N hyperfine splittings (mT) resolved in the EPR spectra of **1a** in toluene at room temperature (Figure S28, Supporting Information). Calculated splittings are averaged for two C_s-symmetric conformations of **1a**, corresponding to 180° rotation of the *tert*-butyl groups. The unresolved splittings are computed to be ≤0.01 mT, and in particular ^{14}N hyperfine splitting for the amine group (NH) is on the order of −0.005 mT (Table S3, Supporting Information).

organic radicals such as **1** and **1a** are primarily determined by the Fermi contact terms (*s*-type spin density at the observed nucleus),[33] the ^{1}H chemical shift of each proton depends on the sign and magnitude of isotropic electron−proton hyperfine coupling constants (or splittings $a_{iso}/2$ for triplet diradical and a_{iso} for doublet monoradical), as well as the diamagnetic contribution to the shift such as the ^{1}H chemical shift in the diamagnetic reference compound such as diamine **2**.

^{1}H NMR spectra of **1** and **1a** were obtained in chloroform-*d* at room temperature. For nitroxide diradical **1**, a broad, intense resonance centered at about 9.0 ppm is observed (Figure S23, Supporting Information).[19] We assign this resonance to protons of the *tert*-butyl groups ($C(CH_3)_3$) and *gem*-dimethyl ($C(CH_3)_2$) groups, for which positive paramagnetic shifts are expected due to the conjugative transfer of positive spin density from the π-conjugated system (nitroxides and corresponding *ortho*/*para* positions) to the methyl hydrogens ("homohyperconjugation"),[39] analogously as in other planar aryl nitroxide diradicals.[13] This assignment is confirmed by the UB3LYP/EPR-III calculations of isotropic ^{1}H hyperfine couplings in **1**, which give ^{1}H chemical shifts of 9.0 and 12.8 ppm for $C(CH_3)_3$ and $C(CH_3)_2$ groups, respectively (Table S2, Supporting Information). For nitroxide monoradical **1a**, several ^{1}H resonances in the (−1)−10 ppm range are observed (Figures S24, S25, and S27, Supporting Information). The UB3LYP/EPR-III calculations of isotropic ^{1}H hyperfine couplings in **1a** indicate that all protons with small, unresolved ^{1}H splittings (≤0.01 mT) in the EPR spectra of **1a** (Figure 2) are predicted to have ^{1}H chemical shifts in the 1−13 ppm range (Table S3, Supporting Information) that is similar to what is observed experimentally.

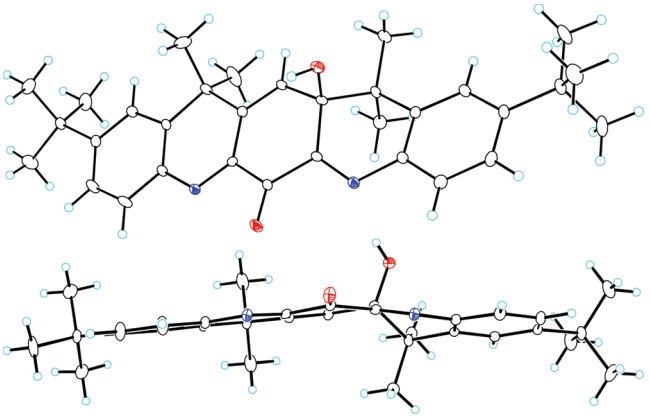

Figure 3. Molecular structure and conformation for **3**, the main product of oxidation of diamine **2** with DMDO. (A) Top view of **3**; (B) side view of **3**. In the top view, carbon, nitrogen, and oxygen atoms are depicted with thermal ellipsoids set at the 50% probability level. The second unique molecule and solvent molecules are omitted for clarity.

Analysis of Diamagnetic Byproducts. *X-ray Structure of* ***3***. Structure of the diamagnetic product **3** obtained from oxidation of **2** with DMDO is established unequivocally by X-ray crystallography (Figure 3). The asymmetric unit consists of two crystallographically unique molecules with opposite configurations at the chiral carbons and three solvent molecules (dichloromethane).[40]

Reaction of ***3*** *with m-CPBA.* Interestingly, we find that **3**, which is isolated from the reaction of diamine **2** with DMDO, reacts with *m*-CPBA (~1 equiv) to give a product that is identical to the major diamagnetic byproduct isolated from oxidation of **2** with *m*-CPBA (**4**, $C_{32}H_{38}N_2O_3$), as well as a minor product **7** that is an isomer of **5**, $C_{31}H_{38}N_2O_2$ (Scheme 4).

In addition, we find that when **4** is loaded on silica gel at ambient conditions, it slowly transforms to a new product, for which both ^{1}H NMR spectra in the aromatic region and R_f values are identical to those for **5**.

Possible Reaction Pathways from ***3*** *to* ***4***, ***5***, ***6***, *and* ***7***. The formation of **4** and **5**, which are diamagnetic byproducts formed in the oxidation of **2** with *m*-CPBA, in the reaction of **3** with *m*-CPBA provides a clue that **3** might be an intermediate in the oxidation of **2**; however, neither **3** nor **7** are detectable in the crude reaction mixtures of such a reaction. We are intrigued to investigate possible transformation pathways from **3** to these products, for which we explore similar transformations in the literature to deduce possible structures in these processes and then verify these structures by computational studies (Scheme 5).

dx.doi.org/10.1021/jo2017923 |*J. Org. Chem.* 2011, 76, 8447–8457

Structure of **3** may be considered to consist of two imine moieties, for which an imine *N*-oxide may be expected as the product from reaction of **3** with *m*-CPBA. A similar example in the literature is the reaction of *N*-phenyl-*p*-quinoneimine with perbenzoic acid in benzene at room temperature (24 h) in subdued light to give brown crystals of the corresponding *N*-oxide (80% yield).[41] However, the spectral data preclude that colorless solid **4** could be an imine *N*-oxide.

Scheme 4. Oxidation of 3 with *m*-CPBA and Transformation of Byproduct 4

The structure of **3** may also be viewed as an unsaturated α-diiminoketone with cross-conjugated C═N and C═O moieties analogous to α-triketones. It is well-known that α-diketones, including unsaturated α-diketones such as *o*-benzoquinones and *o*-naphthoquinones, readily react with Baeyer–Villiger reagents (peroxyacids, etc.) to form cyclic anhydrides in inert solvents.[42−45] That is, the oxygen is preferentially inserted between the carbonyl groups, compared to the less favorable formation of oxacyclopropane or ester.[46,47]

There are only a few reports on reactions of α-iminoketones and their derivatives with peroxy compounds. Among those relevant to this work are reports on preferential insertion of oxygen between the imino and carbonyl groups, analogously as in α-diketones.[43,48,49] Specifically, the reaction of 3-oxo-2-phenylindolenine with *m*-CPBA in chloroform at room temperature produces the corresponding benzoxazine structure (eq 3).[48]

Scheme 5. Proposed Reaction Pathways Leading to Isolated Products 4, 5, 6, and 7[a]

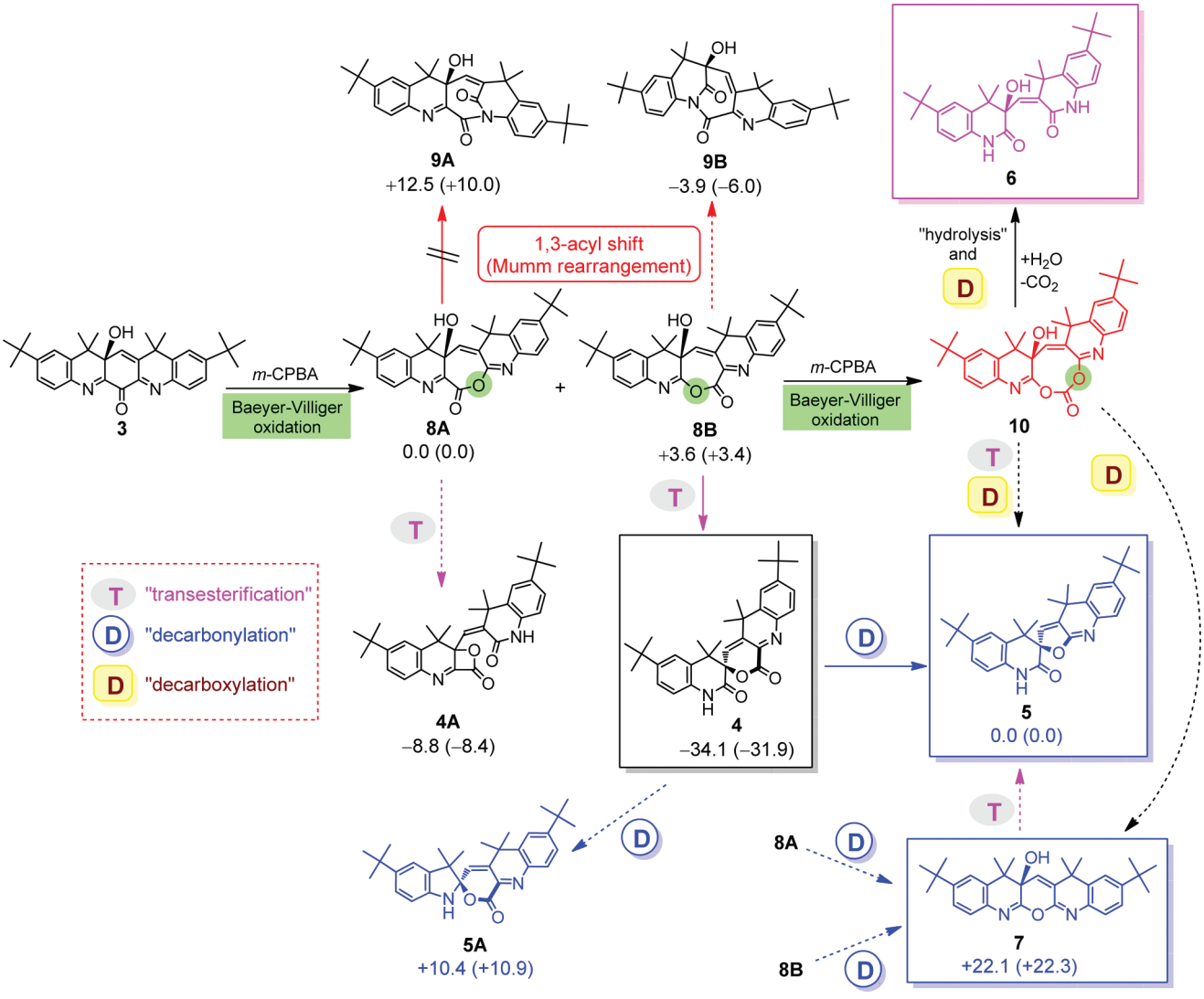

[a] Calculated relative energies (kcal mol^{-1}) in DCM (and in the gas phase) versus **8A** and **5** for the $C_{32}H_{38}N_2O_3$ isomers (black color) and the $C_{31}H_{38}N_2O_2$ isomers (blue color), respectively. For each structure, energies for the lowest energy conformers, which are minima on the potential surface, are shown. For the energies in dichloromethane, B3LYP/6-31G(d,p)/IEF-PCM-UA0//B3LYP/6-31G(d,p)+ZPVE level of theory was used, except for the $C_{31}H_{38}N_2O_2$ isomers (blue color) for which B3LYP/6-31G(d,p)/IEF-PCM-UAHF//B3LYP/6-31G(d,p)+ZPVE level of theory was used. For the energies in the gas phase, B3LYP/6-31G(d,p)//B3LYP/6-31G(d,p)+ZPVE level of theory was used.

dx.doi.org/10.1021/jo2017923 |*J. Org. Chem.* 2011, 76, 8447–8457

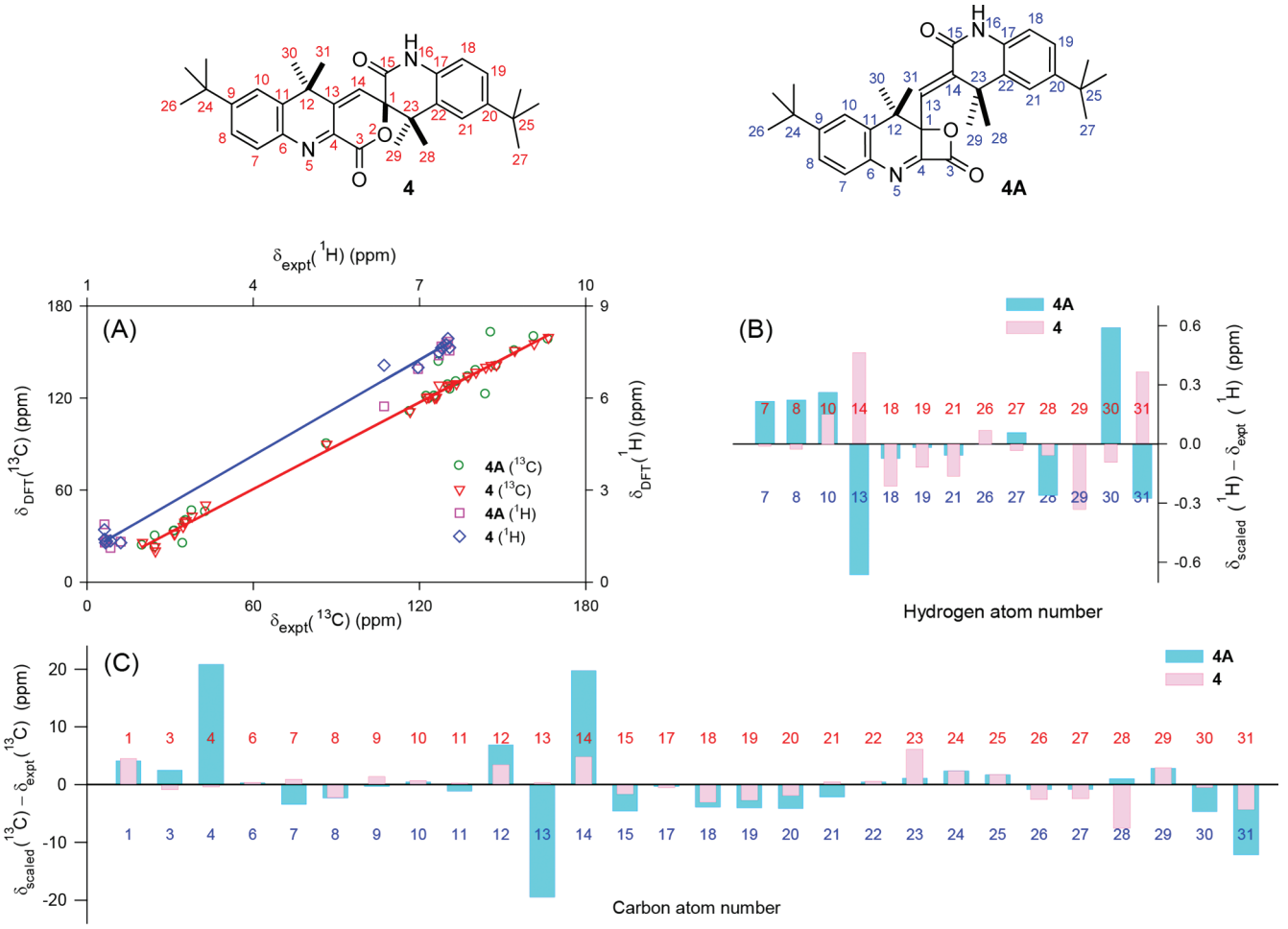

Figure 4. Calculated and experimental ^{1}H and ^{13}C NMR chemical shifts for **4** and **4A**. (A) Correlations between calculated (δ_{DFT}) and experimental (δ_{expt}) ^{1}H and ^{13}C NMR chemical shifts. Solid lines are the best fit to $\delta_{DFT} = a + b\delta_{expt}$ for **4**. (B, C) Difference between scaled ($\delta_{scaled} = (\delta_{DFT} - a)/b$) and experimental ($\delta_{expt}$) ^{1}H and ^{13}C NMR chemical shifts. Statistical parameters are summarized in Table 2.

The significant reactivity of the α-iminoketones in Baeyer–Villiger-like oxidations may be associated with the facile addition of peroxy reagents to the imino moiety, as indicated by the detection of the corresponding tetrahedral intermediates between hydrogen peroxide and 3-oxo-2-arylindolenines.[49]

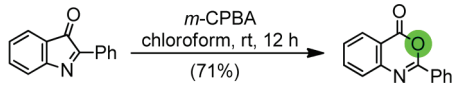

(3)

On the basis of these reports, we postulate that the initial step in the reaction of **3** with *m*-CPBA corresponds to a Baeyer–Villiger-type oxidation, in which the oxygen atom is inserted between the imino and carbonyl groups. Two seven-membered ring constitutional isomers **8A** and **8B** are possible, for which we determine by DFT computations that their lowest energy conformations have similar energies (Scheme 5). It is plausible that **8B** might be preferred under the kinetic control of Baeyer–Villiger oxidation leading to the migration of more hindered group.[50] Because **8A** and **8B** contain an isoimide moiety, the subsequent rearrangement could lead to the corresponding imides **9A** and **9B** via 1,3-shift of the acyl group from oxygen to nitrogen (Mumm rearrangement).[51,52] Alternatively, high reactivity of the carbonyl group in isoimides toward nucleophiles[53] could lead to the acylation of the alcohol moiety ("transesterification") in **8A** and **8B** to provide **4A** and **4**, respectively (Scheme 5).

However, the Mumm rearrangement can be quite slow for cyclic isoimides,[52] and in the case of **8A** and **8B**, the rearrangement could be even less favorable because the products **9A** and **9B** have bicyclic structures, with a bridgehead double bond in **9A**. The low thermodynamic driving force for the rearrangement to **9A** and **9B** is suggested by the DFT-calculated energies for their major conformers, which are 10–13 kcal mol^{-1} above **8A** and 4–6 kcal mol^{-1} below **8B**, respectively. The DFT calculations indicate much more downhill pathways for the intramolecular transesterifications to provide **4A** and **4**, respectively (Scheme 5). In particular, the spirocyclic structure with two six-membered rings such as **4** is >30 kcal mol^{-1} below **8B**. Therefore, we assign this spirocyclic structure to the major isolated byproduct **4**.

We propose that decarbonylation of the α-imino-δ-lactone moiety in **4** provides an isoamide moiety in the spirocyclic product **5**, to account for the experimental observation that **5** is formed directly from **4**. This observation is also supported by the reports of surprising acid-catalyzed decarbonylations of carboxylic acid derivatives,[54] including decarbonylation of a δ-lactone moiety,[55] and the well-known utility of silica gel as an acid catalyst.[56–58] An alternative decarbonylation pathway with loss of CO from the δ-lactam moiety in **4**, to provide another

dx.doi.org/10.1021/jo2017923 |J. Org. Chem. 2011, 76, 8447–8457

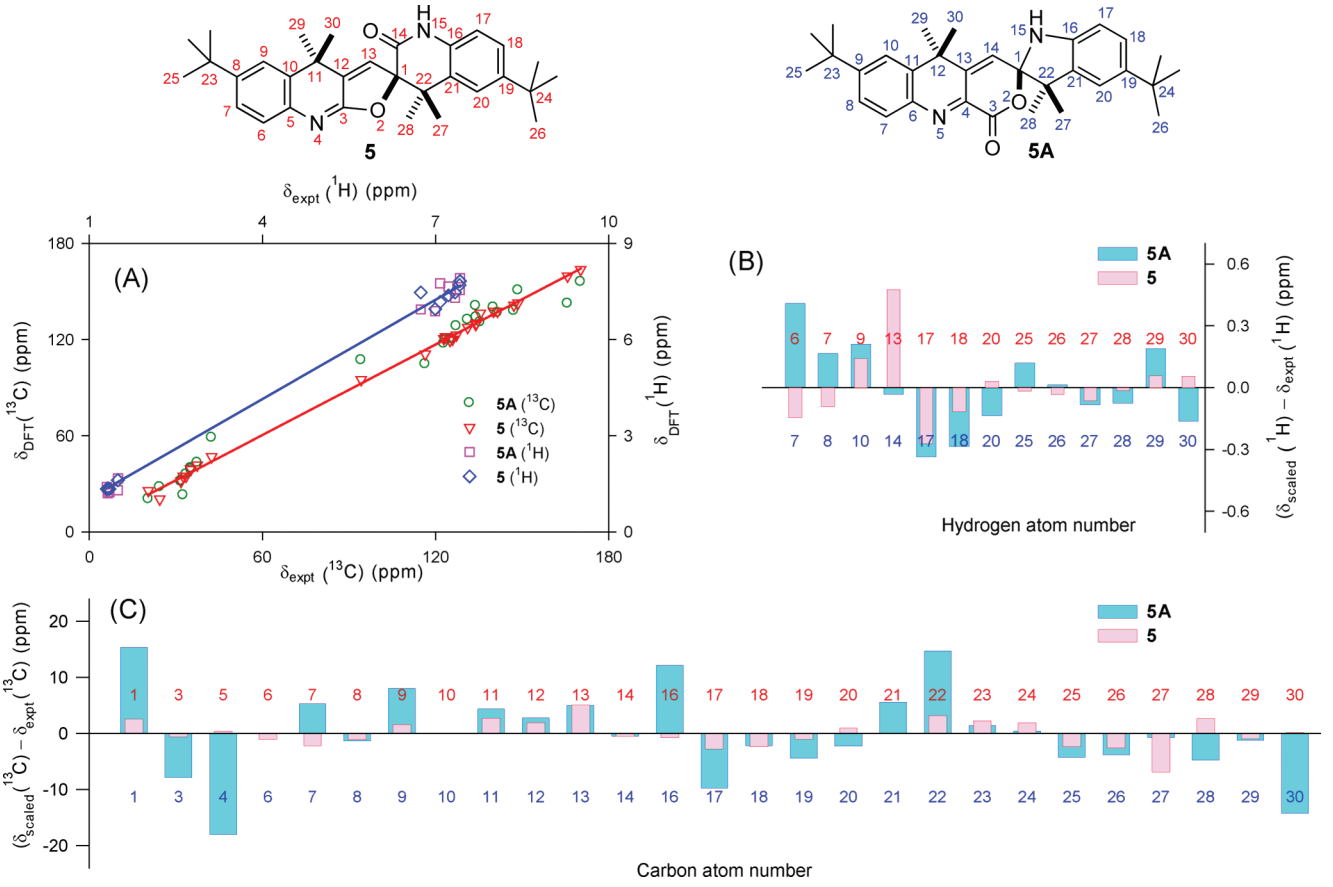

Figure 5. Calculated and experimental ^{1}H and ^{13}C NMR chemical shifts for **5** and **5A**. (A) Correlations between calculated (δ_{DFT}) and experimental (δ_{expt}) ^{1}H and ^{13}C NMR chemical shifts. Solid lines are the best fit to $\delta_{DFT} = a + b\delta_{expt}$ for **5**. (B, C) Difference between scaled ($\delta_{scaled} = (\delta_{DFT} - a)/b$) and experimental ($\delta_{expt}$) ^{1}H and ^{13}C NMR chemical shifts; upper and lower atom numbering corresponds to that for **5** and **5A**, respectively. Statistical parameters are summarized in Table 2.

spirocyclic structure **5A** that is 10 kcal mol^{-1} above **5**, is considered to be less likely.

We consider the possibility that **8A** or **8B** may undergo additional Baeyer−Villiger oxidation with the insertion of oxygen between the imino and carbonyl groups to provide eight-membered ring structures such as **10**. The formation of **10**, followed by hydrolysis and "decarboxylation", may provide a pathway toward the minor byproduct **6** (Scheme 5).

It is plausible that intramolecular transesterification and/or decarboxylation of **10** might provide alternative pathways to the byproduct **5** as well as the minor byproduct **7**, which also might possibly form via decarbonylation of either **8A** or **8B** (Scheme 5).

*Structure Determination for Diamagnetic Byproducts **4**, **5**, **6**, and **7** Using NMR Spectroscopy.* Spirocyclic structures of major byproducts **4** and **5** are confirmed by the assignment of their experimental ^{1}H and ^{13}C NMR spectra in acetone-d_6 using standard 2D NMR spectroscopy, including ^{1}H−^{13}C HSQC, ^{1}H−^{13}C HMBC, ^{1}H−^{1}H NOESY, and ^{1}H−^{15}N HSQC. The detection of ^{1}H−^{15}N HSQC cross-peak between ^{1}H at δ = 9.62 ppm and ^{15}N at δ = −250 ppm (relative to nitromethane at 0.0 ppm) for **4** and between ^{1}H at δ = 9.52 ppm and ^{15}N at δ = −248 ppm for **5** unambiguously establishes the presence of the NH group in the amide (lactam) moiety in each compound. This NH group provides an anchor for the assignment of remaining hydrogens and carbons, as detailed in the Supporting Information (Section 7). For byproduct **4**, the presence of the amide-type NH group limits the possible structures to spirocyclic **4** or four-membered ring **4A** and specifically precludes other structures such as **8A**, **8B**, **9A**, and **9B** that are devoid of the amide or lactam moieties (Scheme 5). For **5**, an alternative spirocyclic structure with an NH moiety such as **5A** that could possibly be formed via decarbonylation of the lactam moiety in **4** (Scheme 5) is less likely because of the observed ^{15}N NMR chemical shifts.

Additional evidence in support of spirocyclic structures **4** and **5** is obtained from the correlation between the DFT-calculated and experimental ^{1}H and ^{13}C NMR chemical shifts.

^{1}H and ^{13}C NMR isotropic shieldings for **4**, **5**, **4A**, **5A**, and tetramethylsilane are computed using the GIAO/B3LYP/6-31G(d,p) level of theory with the IEF-PCM-UA0 solvent model for acetone (Gaussian 03), to provide calculated ^{1}H and ^{13}C NMR chemical shifts δ_{DFT}(^{1}H) and δ_{DFT}(^{13}C) for direct comparison with the experimental NMR spectra in acetone-d_6.[59] As the IEF-PCM solvent model does not properly account for specific solvent−solute interactions such as hydrogen bonding,[60] the protons of NH moieties are not included in the analyses.

For **4** and **5**, the correlations between DFT-computed and experimental NMR chemical shifts give correlation coefficients (R^2) that are expected for correctly assigned structures of medium sized organic molecules (Figures 4A and 5A, Table 2).[28,61] Moreover, the alternative structure assignments **4A** and **5A** have lower values of R^2, especially for ^{13}C NMR chemical shifts (Table 2).

dx.doi.org/10.1021/jo2017923 |*J. Org. Chem.* 2011, 76, 8447–8457

Table 2. Statistical Parameters for the Correlations of ^{1}H and ^{13}C NMR Chemical Shifts[a]

	^{1}H					^{13}C				
structure	*a*	*b*	R^2	MaxErr	CMAE	*a*	*b*	R^2	MaxErr	CMAE
4	−0.0453	1.0413	0.9948	0.4630	0.1610	4.0738	0.9422	0.9969	6.1112	2.2001
4A	−0.0484	1.0137	0.9901	0.6629	0.2078	3.5507	0.9534	0.9794	20.8189	4.5883
5	0.0085	1.0327	0.9966	0.4753	0.1165	4.0036	0.9407	0.9978	6.8853	1.8818
5A	−0.0960	1.0482	0.9950	0.4097	0.1706	5.9911	0.9234	0.9785	18.0399	5.5763

[a] *a* and *b* are the intercept and slope of the linear fit to $\delta_{DFT} = a + b\delta_{expt}$, and R^2 is its correlation coefficient. MaxErr is the maximum corrected absolute error with respect to the linear fit ($|\delta_{scaled} - \delta_{expt}|$). CMAE is the corrected mean absolute error for *n* chemical shifts ($(\Sigma|\delta_{scaled} - \delta_{expt}|/n)$).

The relationship between computed and experimental NMR chemical shifts is further illustrated by applying the correlations to scale linearly $\delta_{DFT}(^{1}H)$ and $\delta_{DFT}(^{13}C)$, to provide $\delta_{scaled}(^{1}H)$ and $\delta_{scaled}(^{13}C)$, and then plot the differences between the scaled and experimental NMR chemical shifts for each distinct carbon and hydrogen atom in the structure (Figures 4B,C and 5B, C).[29,62] These plots clearly suggest that structural assignments for **4** and **5** possess better agreement with the theory than the alternative constitutional isomers **4A** and **5A**, respectively. This conclusion is further supported by low values for statistical parameters such as (MaxErr) and (CMAE) for **4** and **5** (Table 2), as expected for correctly assigned structures. As expected, overall agreement between the theory and experiment is somewhat better for ^{13}C versus ^{1}H NMR chemical shifts.[28,61]

NMR spectroscopic characterization of the minor byproducts **6** and **7** was hindered by their limited availability. Also, the spectra of **6** are broadened. ^{1}H NMR spectra of byproducts **3**, **4**, **5**, **6**, and **7** indicate structural similarities such as two AMX (or ABX) spin coupling systems for 4-*tert*-butyl-substituted benzene rings are observed, which implies that these two benzene rings are intact after oxidation. Each compound has 2 distinct *gem*-dimethyl moieties with diastereotopic methyl groups (4 different methyl groups) and 2 distinct *tert*-butyl groups. The sole exchangeable proton in **7** and in **3** has ^{1}H chemical shift in the 5−6 ppm range (acetone-d_6), as expected for tertiary alcohols of similar structure; analogous proton in **6** could not be unequivocally assigned due to spectral broadening. The exchangeable protons of the NH groups in the lactam moieties of **4**, **5**, and **6** have similar ^{1}H chemical shifts in the 9.0−9.8 ppm range (acetone-d_6). The presence of these NH groups is confirmed by $^{1}H-^{15}N$ HSQC experiments as already described for **4** and **5**; despite spectral broadening for **6**, two $^{1}H-^{15}N$ HSQC cross-peaks could be detected between ^{1}H at δ = 9.76 and 9.00 ppm and ^{15}N at δ = −251 and −241 ppm, respectively (Figure S55, Supporting Information). These ^{15}N NMR chemical shifts for **4**, **5**, and **6** are within the typical range for NH groups in amides, and also, DFT-calculated ^{15}N NMR chemical shifts for these NH groups are within 3 ppm of the experimental values (Table S9, Supporting Information).

Experimental and Computed UV−vis Absorption Spectra. UV−vis spectrum of **3** is obtained in heptane, while the spectra of relatively polar **4** and **5** are recorded in acetonitrile. The computed UV−vis spectra are obtained at the TD-B3LYP/6-31G(d,p) level of theory with the IEF-PCM solvent model for heptane or acetonitrile for direct comparison with the experimental UV−vis spectra. The computed spectra for the proposed structures **3**, **4**, and **5** qualitatively reproduce the observed experimental spectral pattern of three major bands for **3** and two major bands for **4** and **5** in the 220−600 nm range but with slightly red shift of the bands at the longest wavelengths.[30] The agreement between the computed UV−vis spectra for structures **4A** and **5A** and the experiment is less satisfactory (Figure 6), and thus these structures are excluded and the structural assignments of **4** and **5** by the NMR spectroscopy are affirmed.

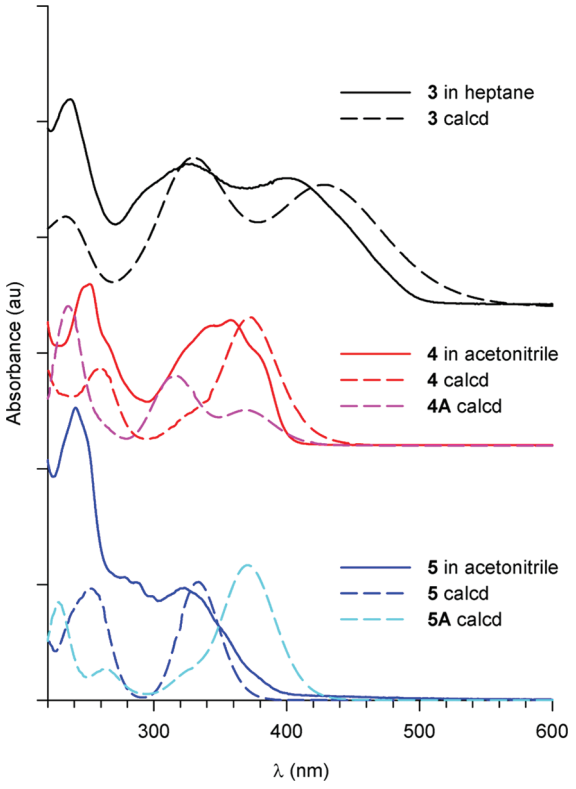

Figure 6. UV−vis absorption spectra: experiment (solid lines) and theory (dashed lines). The spectra are shifted vertically for clarity.

CONCLUSION

Oxidation of annelated diaryl diamine provides paramagnetic products such as nitroxide diradical **1** and monoradical and diamagnetic byproducts. DFT-computed tensors for EPR spectra and paramagnetic ^{1}H NMR isotropic shifts for nitroxide diradical **1** show good agreement with the experimental EPR spectra in rigid matrices and paramagnetic ^{1}H NMR spectra in solution, respectively. Diamagnetic byproducts are formed via distinct pathways involving C−O bond-forming reactions, including Baeyer−Villiger-type oxidations. Consequently, the yields of nitroxide radicals were relatively low, ca. 40% per diarylamine even under carefully optimized conditions, providing corresponding

dx.doi.org/10.1021/jo2017923 |J. Org. Chem. 2011, 76, 8447–8457

nitroxide diradical **1** in about 20% yield. Structures of two of the major diamagnetic products with spirocyclic structures are confirmed by correlations between DFT-computed and experimental ^{13}C and ^{1}H NMR chemical shifts.

EXPERIMENTAL SECTION

Typical Procedure for Oxidation of Diamine 2 with DMDO. DMDO (0.143 M, 1.36 mL, 0.194 mmol) in acetone at 0 °C was vacuum transferred to diamine **2** (20.0 mg, 0.0442 mmol) in degassed dichloromethane in a Schlenk tube at −78 °C, and the greenish yellow reaction mixture was allowed to attain −20 °C. After 2 h at −20 °C, the reddish orange reaction mixture was concentrated *in vacuo*. The resultant yellow/brown crude product (22.8 mg) was purified by column chromatography (silica, DCM/ether, 7:3, ambient temperature), and then PTLC (silica, DCM/ether, 7:3, 0 °C), to provide compound **3** (8.5 mg, 40%) as a yellow solid.

Compound 3. R_f = 0.19 (DCM/ether, 4:1). Mp > 200 °C. (dec, under argon). ^{1}H NMR (400 MHz, acetone-d_6): δ 7.661 (d, J = 2.0 Hz, 1H), 7.612 (d, J = 2.0 Hz, 1H), 7.521 (d, J = 8.0 Hz, 1H), 7.514 (d, J = 8.0 Hz, 1H), 7.437 (dd, J = 2.0, 8.0 Hz, 1H), 7.417 (dd, J = 2.0, 8.0 Hz, 1H), 6.858 (s, 1H), 5.095 (s, 1H, exch D_2O), 1.733 (s, 3H), 1.604 (s, 3H), 1.578 (s, 3H), 1.371 (s, 9H), 1.369 (s, 9H), 0.958 (s, 3H). ^{13}C and ^{1}H NMR spectra in chloroform-*d*, see Supporting Information. HR-EIMS: 482.2935 $[M]^+$ (−0.4 ppm for $^{12}C_{32}{}^{1}H_{38}{}^{14}N_2{}^{16}O_2$). IR ($cm^{-1}$): 3367, 3065, 2961, 2925, 2867, 1698, 1559, 1548, 1463, 1363, 1030, 1001, 836. UV−vis (heptane), λ_{max}/nm (ε_{max}/L mol^{-1} cm^{-1}): 239 (~9 × 10^3), 328 (~6 × 10^3), 402 (~6 × 10^3).

General Procedure for Oxidations of Diamine 2 with 2, 4, and 6 equiv of *m*-CPBA in DCM or Benzene. A solution of purified and dried *m*-CPBA[14,19] (2 equiv, potential hazard[63]) was slowly added to a solution of diamine **2** (1 equiv) at 0 °C (dry DCM as solvent, vacuum transferred) or 6 °C (dry benzene as solvent, vacuum transferred) under nitrogen atmosphere. After 20 min, the reaction mixture was concentrated in vacuo at 0 °C (DCM as solvent) or 6 °C (benzene as solvent), to provide crude product. (For reactions with 4 and 6 equiv of *m*-CPBA, additional 2-equiv portions of *m*-CPBA were slowly added.) The crude product was filtered through silica gel plug at 0 °C using DCM/ether (95:5), to provide the major less polar fraction containing nitroxide radicals, and then DCM/ether (1:2), followed by DCM/MeOH (4:1), to collect more polar fraction containing diamagnetic products.

Alternatively, the crude reaction mixture was filtered through silica plug at room temperature (benzene/ether, 95:5) to provide the major less polar fraction ($R_f \approx 0.4$) containing nitroxide radicals; subsequent PTLC separations (silica, benzene/ether, 98:2 and DCM/ether, 98:2) gave diradical **1** (when 6 equiv of *m*-CPBA was used) and monoradical **1a**.

The more polar fraction was dissolved in DCM, washed with pH 7.4 phosphate buffer, dried over Na_2SO_4, and then concentrated. Purification by PTLC at 0 °C provided diamagnetic byproducts; when 6 equiv of *m*-CPBA in DCM was used the isolated yields were as follows: **4** (14%), **5** (9%), and **6** (4%).

Oxidation of diamine 2 with Na_2WO_4/H_2O_2. Diamine **2** (50.0 mg, 0.110 mmol), Na_2WO_4-dihydrate (72.5 mg, 0.220 mmol), Me_3N-($C_{12}H_{25}$)Cl (16.9 mg, 0.055 mmol), hydrogen peroxide (35 wt %, 2.0 mL), and DCM (12 mL) were stirred for 14 h at room temperature. The reaction mixture was filtered and concentrated under vacuo to provide crude product (70.7 mg). PTLC (silica, DCM/ether, 15:1) provided two main fractions that were EPR active; the more polar fraction corresponded to nitroxide monoradical **1a** with a small admixture of diradical **1** (17.8 mg, ~30%) and the less polar fraction corresponded to radical **1b** (21.1 mg).

Subsequent oxidation of **1a** (5.1 mg, 0.011 mmol) with *m*-CPBA (4.75 mg, 2.5 equiv) in DCM (4 mL, vacuum transferred) under nitrogen atmosphere overnight gave a low yield of nitroxide diradical **1** (~0.5 mg, ~10%).

Nitroxide Diradical 1[19]**.** ^{1}H NMR (500 MHz, 7.3 mg of **1** in 0.5 mL of chloroform-*d*): δ ~9.0 (br s).

Nitroxide Monoradical 1a. EPR (X-band, toluene, 295 K): g_{iso} = 2.0051. ^{1}H NMR (500 MHz, 3.5 mg of **1a** in 0.5 mL of chloroform-*d*): δ ~8.77 (br s), 7.760 (s), 6.110 (s), 1.295 (s), −0.68 (br s). IR (cm^{-1}): 3377, 2966, 2927, 2869, 1612, 1506, 1459, 1413, 1361, 1326, 817.

Compound 4. R_f = 0.63 (DCM/MeOH, 25:1 at 0 °C). Purified by PTLC (silica) at 0 °C, using DCM/MeOH (96:4), to provide the product as a white solid (R_f = 0.34 in DCM/MeOH, 95:5). Mp 239−240 °C (under air). ^{1}H NMR (400 MHz, acetone-d_6): δ 9.620 (br s, 0.8H, exch D_2O), 7.546 (d, J = 2.0 Hz, 1H), 7.514 (d, J = 2.0 Hz, 1H), 7.483 (d, J = 8.4 Hz, 1H), 7.398 (dd, J = 2.0, 8.0 Hz, 1H), 7.352 (dd, J = 2.0, 8.0 Hz, 1H), 6.974 (d, J = 8.4 Hz, 1H), 6.363 (s, 1H), 1.607 (s, 3H), 1.425 (s, 3H), 1.355 (s, 9H), 1.335 (s, 3H), 1.317 (s, 9H), 1.216 (s, 3H). ^{13}C NMR (100 MHz, acetone-d_6, $^{1}H-^{13}C$ HMQC cross-peak at 500/125 MHz): δ 166.6 (q), 161.4 (q), 154.5 (q), 147.8 (q), 145.9 (q), 144.0 (q), 140.4 (q), 137.6 (q), 133.4 (q), 131.1 (7.483), 130.4 (q), 127.1 (6.363), 126.2 (7.352), 125.5 (7.398), 123.4 (7.546), 122.6 (7.514), 116.6 (6.974), 86.5 (q), 42.8 (q), 32.9 (q), 35.8 (q), 35.3 (q), 34.7 (1.216), 31.8 (1.355), 31.5 (1.317), 24.7 (1.335), 24.6 (1.425), 20.1 (1.607). HR-EIMS: 498.2883 $[M]^+$ (−0.2 ppm for $^{12}C_{32}{}^{1}H_{38}{}^{14}N_2{}^{16}O_3$). IR ($cm^{-1}$): 3238, 3066, 2963, 2929, 2869, 1758, 1698, 1506, 1463, 1366. UV−vis (acetonitrile), λ_{max}/nm (ε_{max}/L mol^{-1} cm^{-1}): 252 (~2.5 × 10^4), 358 (~2 × 10^4).

Compound 5. R_f = 0.51 (DCM/MeOH, 25:1 at 0 °C). Purified by PTLC (silica) at 0 °C, using pentane/ether (8:2), to provide the product as a white solid with blue fluorescence (R_f = 0.28 in DCM/MeOH, 95:5). Mp 334 °C (under air). ^{1}H NMR (400 MHz, acetone-d_6): δ 9.525 (br s, 0.2−1.0H), 7.453 (d, J = 2.4 Hz, 1H), 7.419 (d, J = 2.4 Hz, 1H), 7.334 (dd, J = 2.0, 8.4 Hz, 1H), 7.219 (dd, J = 2.0, 8.4 Hz, 1H), 7.081 (d, J = 8.0 Hz, 1H), 6.993 (d, J = 8.4 Hz, 1H), 6.748 (s, 1H), 1.498 (s, 3H), 1.494 (s, 3H), 1.351 (s, 3H), 1.328 (s, 12H), 1.304 (s, 9H), 1.194 (s, ~1.5H, impurity, $^{1}H-^{13}C$ HMQC cross-peak to ^{13}C resonance overlapped with acetone-d_6). ^{13}C NMR (100 MHz, acetone-d_6, $^{1}H-^{13}C$ HMQC cross-peak at 500/125 MHz): δ 170.3 (q), 165.8 (q), 148.7 (q), 147.1 (q), 141.5 (q), 140.1 (q), 135.5 (6.748), 134.15 (q), 133.95 (q), 131.19 (q), 127.20 (7.081), 125.90 (7.334), 125.09 (7.219), 124.46 (7.453), 122.88 (7.419), 116.43 (6.993), 94.20, 42.4 (q), 37.4 (q), 35.22 (q), 35.16 (q), 33.6 (1.494), 32.6 (1.498), 31.82 (1.328), 31.77 (1.304), 24.5 (br, 1.351), 20.6 (br, 1.328). HR-EIMS: 470.2931 $[M]^+$ (0.5 ppm for $^{12}C_{31}{}^{1}H_{38}{}^{14}N_2{}^{16}O_2$). IR ($cm^{-1}$): 3241, 3147, 3060, 2962, 2930, 2869, 1703, 1664, 1505, 1487, 1462, 1363, 1350, 1257, 1043. UV−vis (acetonitrile), λ_{max}/nm (ε_{max}/L mol^{-1} cm^{-1}): 242 (~2 × 10^4), 324 (~8 × 10^3).

Compound 6. R_f = 0.32 (DCM/MeOH, 25:1 at 0 °C). Purified by PTLC (silica) at 0 °C, using DCM/MeOH (25:1), to provide the product as a glassy film. ^{1}H NMR (400 MHz, acetone-d_6): δ 9.76 (br s, 1H, exch D_2O), 9.00 (br s, 1H, exch D_2O), 7.402 (d, J = 2.1 Hz, 1H), 7.31 (br s, 1H), 7.249 (dd, J = 8.4, 2.0 Hz, 1H), 7.224 (dd, J = 8.3, 2.1, 1H), 6.967 (d, J = 8.4 Hz, 1H), 6.816 (d, J = 8.3 Hz, 1H), 6.101 (br s, 1H), 1.16−1.38 (br. m, 12 H), 1.315 (s, 9H), 1.268 (s, 9H). ^{13}C NMR: not obtained due to resonance broadening. HR-FABMS (3-NBA matrix): m/z ion type (percent relative amplitude for m/z 486−492, deviation from formula), 490.3136 $[M + H + 1]^+$ (35, +3.1 ppm for $^{12}C_{30}{}^{13}C_1{}^{1}H_{41}{}^{14}N_2{}^{16}O_3$), 489.3100 $[M + H]^+$ (100, +3.5 ppm for $^{12}C_{31}{}^{1}H_{41}{}^{14}N_2{}^{16}O_3$), 488.3009 $[M]^+$ (12, +6.0 ppm for $^{12}C_{31}{}^{1}H_{40}{}^{14}N_2{}^{16}O_3$). IR ($cm^{-1}$): 3430, 3209, 2960, 2932, 2870, 1685, 1663, 1558, 1505, 1395, 1363, 827, 761, 741.

Oxidation of Compound 3 with *m*-CPBA: Formation of 4 and 7. A solution of *m*-CPBA (0.07 M, 39 μL, 2.7 μmol) in DCM was slowly added to a stirred solution of **3** (1.3 mg, 2.7 μmol) in DCM (0.4 mL) at 0 °C. After 3 h at 0 °C, the green yellow reaction mixture was

dx.doi.org/10.1021/jo2017923 |*J. Org. Chem.* 2011, 76, 8447–8457

washed with pH 7.4 phosphate buffer and after further aqueous workup separated by PTLC (deactivated silica, DCM/ether, 10:1), to provide **4** as a pale yellow solid (~0.9 mg), **7** as a pale yellow film (~0.4 mg, ~30%), and the starting material **3** (~0.3 mg).

Compound 7. R_f = 0.66 (DCM/ether, 4:1). ^{1}H NMR (500 MHz, acetone-d_6, aromatic region, Figure S60, Supporting Information): δ 8.064 (d, J = 8.0 Hz, 0.78 H), 7.624 (d, J = 2.0 Hz, 1 H), 7.499 (d, J = 8.0 Hz, 1 H), 7.409 (dd, J = 2.0, 8.5 Hz, 1 H), 7.403 (d, J = 1.5 Hz, 1 H, LB = −0.6 Hz, GB = 0.3), 7.335 (dd, J = 2.0, 8.5 Hz, 1 H), 6.859 (s, 1 H), 5.625 (s, 0.14 H, DCM) 5.615 (s, 0.48 H, exch D_2O), 5.5−5.3 (m, 0.73 H, impurity). Aliphatic region consists of 4 different methyl groups and 2 different *tert*-butyl groups, as well as the vacuum grease impurity. LR/HR-FABMS (3-NBA matrix): m/z ion type (percent relative amplitude for m/z 400−600, deviation for the formula): 471.2999 $[M + H]^+$ (100, 2.6 ppm for $^{12}C_{31}{}^{1}H_{39}{}^{14}N_2{}^{16}O_2$), 472.3039 $[M + H + 1]^+$ (38, 1.3 ppm for $^{12}C_{30}{}^{13}C_1{}^{1}H_{39}{}^{14}N_2{}^{16}O_2$).

Formation of 5 from 4. Compound **4** (5.9 mg, 1.2 μmol) was applied to a PTLC plate (silica) and then developed with diethyl DCM/ether (4:1) to ~16 mm height. After 20 h at ambient conditions, the plate was further developed, to provide after extraction a first portion of **5** (0.5 mg). The unreacted **4** was left on the plate for 48 h at ambient conditions and after additional TLC separation provided another portion of **5** (total 1.9 mg, ~30%).

■ ASSOCIATED CONTENT

Supporting Information. Complete ref 36, general procedures and materials, additional experimental and computational details, and X-ray crystallographic file in CIF format. This material is available free of charge via the Internet at http://pubs.acs.org.

■ AUTHOR INFORMATION

Corresponding Author

*E-mail: arajca1@unl.edu.

Present Addresses

[§]Faculty of Chemistry, Wrocław University of Technology, Wyspiańskiego 27, 50-370 Wrocław, Poland.

■ ACKNOWLEDGMENT

We thank the National Science Foundation for support of this research (CHE-0414936, CHE-0718117, and CHE-1012578), including the purchase of the EPR spectrometer (DMR-0216788) used in this work, and the Air Force Office of Scientific Research (FA9550-04-1-0056). ChemMatCARS Sector 15 is principally supported by the National Science Foundation/Department of Energy under grant number CHE-0087817. The Advanced Photon Source is supported by the U.S. Department of Energy, Basic Energy Sciences, Office of Science, under Contract No. W-31-109-Eng-38. We thank Arnon Olankitwanit for NMR experiments on compound **6** and Dr. Ying Wang for retaking UV−vis absorption spectra of compounds **4** and **5**.

■ REFERENCES

(1) Tretyakov, E. V.; Ovcharenko, V. I. *Russ. Chem. Rev.* **2009**, *78*, 971–1012.

(2) Yamakoshi, H.; Shibuya, M.; Tomizawa, M.; Osada, Y.; Kanoh, N; Iwabuchi, Y. *Org. Lett.* **2010**, *12*, 980–983.

(3) (a) Koshika, K.; Sano, N.; Oyaizu, K.; Nishide, H. *Chem. Commun.* **2009**, 836–838. (b) Nishide, H.; Oyaizu, K. *Science* **2008**, *319*, 737–738.

(4) Suzuki, S.; Furui, T.; Kuratsu, M.; Kozaki, M.; Shiomi, D.; Sato, K.; Takui, T.; Okada, K. *J. Am. Chem. Soc.* **2010**, *132*, 15908–15910.

(5) Goldstein, S.; Samuni, A.; Hideg, K.; Merenyi, G. *J. Phys. Chem. A* **2006**, *110*, 3679–3685.

(6) Burks, S. R.; Bakhshai, J.; Makowsky, M. A.; Muralidharan, S.; Tsai, P.; Rosen, G. M.; Kao, J. P. Y. *J. Org. Chem.* **2010**, *75*, 6463–6467.

(7) Hawker, C. J.; Bosman, A. W.; Harth, E. *Chem. Rev.* **2001**, *101*, 3661–3688.

(8) Mediator of charge recombination in donor-bridge-acceptor systems: Chernick, E. T.; Mi, Q.; Kelley, R. F.; Weiss, E. A.; Jones, B. A.; Marks, T. J.; Ratner, M. A.; Wasielewski, M. R. *J. Am. Chem. Soc.* **2006**, *128*, 4356–4364.

(9) Kirk, M. L.; Shultz, D. A.; Schmidt, R. D.; Habel-Rodriguez, D.; Lee, H.; Lee, J. *J. Am. Chem. Soc.* **2009**, *131*, 18304–18313.

(10) Rajca, A.; Kathirvelu, V.; Roy, S. K.; Pink, M.; Rajca, S.; Sarkar, S.; Eaton, S. S.; Eaton, G. R. *Chem.—Eur. J.* **2010**, *16*, 5778–5782.

(11) (a) Forrester, A. R.; Hay, J. M.; Thomson, R. H. *Organic Chemistry of Stable Free Radicals*; Academic Press: London, 1968; Chapter 5, pp 180−246. (b) Volodarsky, L. B.; Reznikov, V. A.; Ovcharenko, V. I. *Synthetic Chemistry of Stable Nitroxides*; CRC Press: Boca Raton, FL, 1994.

(12) Murray, R. W.; Singh, M. *Tetrahedron Lett.* **1988**, *29*, 4677–4680.

(13) Rajca, A.; Takahashi, M.; Pink, M.; Spagnol, G.; Rajca, S. *J. Am. Chem. Soc.* **2007**, *129*, 10159–10170.

(14) (a) Rajca, A.; Vale, M.; Rajca, S. *J. Am. Chem. Soc.* **2008**, *130*, 9099–9105. (b) Vale, M.; Pink, M.; Rajca, S.; Rajca, A. *J. Org. Chem.* **2008**, *73*, 27–35.

(15) Ivanov, Y. A.; Kokorin, A. I.; Shapiro, A. B.; Rozantsev, E. G. *Izv. Akad. Nauk SSSR, Ser. Khim.* **1976**, *10*, 2217–2222.

(16) Delen, Z.; Lahti, P. M. *J. Org. Chem.* **2006**, *71*, 9341–9347.

(17) Seino, M.; Akui, Y.; Ishida, T.; Nogami, T. *Synth. Met.* **2003**, *133−134*, 581–583.

(18) Nitroxide triradicals and polyradicals containing diarylnitroxide moiety: (a) Ishida, T.; Iwamura, H. *J. Am. Chem. Soc.* **1991**, *113*, 4238–4241. (b) Tanaka, M.; Matsuda, K.; Itoh, T.; Iwamura, H. *J. Am. Chem. Soc.* **1998**, *120*, 7168–7173. (c) Oka, H.; Kouno, H.; Tanaka, H. *J. Mater. Chem.* **2007**, *17*, 1209–1215.

(19) Rajca, A.; Shiraishi, K.; Rajca, S. *Chem. Commun.* **2009**, 4372–4374.

(20) Barone, V.; Cacelli, I.; Ferretti, A.; Monti, S.; Prampolini, G. *Phys. Chem. Chem. Phys.* **2011**, *13*, 4709–4714.

(21) (a) Herrmann, C.; Solomon, G. C.; Ratner, M. A. *J. Am. Chem. Soc.* **2010**, *132*, 3682–3684. (b) Giacobbe, E. M.; Mi, Q.; Colvin, M. T.; Cohen, B.; Ramanan, C.; Scott, A. M.; Marks, T. J.; Ratner, M. A.; Wasielewski, M. R. *J. Am. Chem. Soc.* **2009**, *131*, 3700–3712. (c) Komatsu, H.; Matsushita, M. M.; Yamamura, S.; Sugawara, Y.; Suzuki, K.; Sugawara, T. *J. Am. Chem. Soc.* **2010**, *132*, 4528–4529.

(22) Triarylmethyl and aminyl diradicals based upon tetrahydropentacene and tetrahydrodiazapentacene cores: (a) Rajca, A.; Utamapanya, S. *J. Org. Chem.* **1992**, *57*, 1760–1767. (b) Rajca, A.; Shiraishi, K.; Pink, M.; Rajca, S. *J. Am. Chem. Soc.* **2007**, *129*, 7232–7233. (c) Boratyński, P. J.; Pink, M.; Rajca, S.; Rajca, A. *Angew. Chem., Int. Ed.* **2010**, *49*, 5459–5462.

(23) Reviews on high-spin polyradicals: (a) Iwamura, H.; Koga, N. *Acc. Chem. Res.* **1993**, *26*, 346–351. (b) Rajca, A. *Chem. Rev.* **1994**, *94*, 871–893. (c) *Magnetic Properties of Organic Materials*; Lahti, P. M., Ed.; Marcel Dekker: New York, 1999; pp 1−713. (d) *Molecular Magnetism*; Itoh, K.; Kinoshita, M., Eds.; Gordon and Breach: Kodansha, 2000; pp 1−337. (e) Rajca, A. *Chem.—Eur. J.* **2002**, *8*, 4834–4841. (f) Rajca, A. *Adv. Phys. Org. Chem.* **2005**, *40*, 153–199. (g) Shishlov, N. M. *Russ. Chem. Rev.* **2006**, *75*, 863–884.

(24) (a) Rajca, A.; Wongsriratanakul, J.; Rajca, S. *Science* **2001**, *294*, 1503–1505. (b) Rajca, A.; Rajca, S.; Wongsriratanakul, J. *J. Am. Chem. Soc.* **1999**, *121*, 6308–6309.

(25) (a) Rajca, S.; Rajca, A.; Wongsriratanakul, J.; Butler, P.; Choi, S. *J. Am. Chem. Soc.* **2004**, *126*, 6972–6986. (b) Rajca, A.; Wongsriratanakul, J.; Rajca, S. *J. Am. Chem. Soc.* **2004**, *126*, 6608–6626. (c) Rajca, A.; Wongsriratanakul, J.; Rajca, S.; Cerny, R. L. *Chem.—Eur. J.* **2004**,

10, 3144–3157. (d) Rajca, A.; Lu, K.; Rajca, S. *J. Am. Chem. Soc.* **1997**, *119*, 10335–10345. (e) Rajca, A.; Rajca, S.; Padmakumar, R. *Angew. Chem., Int. Ed. Engl.* **1994**, *33*, 2091–2093. (f) Rajca, A. *J. Am. Chem. Soc.* **1990**, *112*, 5890–5892. (g) Rajca, A. *J. Am. Chem. Soc.* **1990**, *112*, 5889–5890.

(26) Shiraishi, K.; Rajca, A.; Pink, M.; Rajca, S. *J. Am. Chem. Soc.* **2005**, *127*, 9312–9313.

(27) Reaction mixtures from oxidation with 6, 4, or 2 equiv of 4-methoxyperbenzoic acid have diamagnetic components similar to those from oxidation with *m*-CPBA, but diradical **1** could not be detected by ^{1}H NMR spectroscopy.

(28) Jain, R.; Bally, T.; Rablen, P. R. *J. Org. Chem.* **2009**, *74*, 4017–4023.

(29) Saielli, G.; Nicolaou, K. C.; Ortiz, A.; Zhang, H.; Bagno, A. *J. Am. Chem. Soc.* **2011**, *133*, 6072–6077.

(30) Jacquemin, D.; Perpéte, E. A.; Ciofini, I.; Adamo, C. *Acc. Chem. Res.* **2009**, *42*, 326–334.

(31) Sinnecker, S.; Neese, F. *J. Phys. Chem. A* **2006**, *110*, 12267–12275.

(32) Neese, F. *J. Chem. Phys.* **2001**, *115*, 11080–11096.

(33) Rastrelli, F.; Bagno, A. *Chem.—Eur. J.* **2009**, *15*, 7990–8004.

(34) Rajca, A.; Olankitwanit, A.; Rajca, S. *J. Am. Chem. Soc.* **2011**, *133*, 4750–4753.

(35) Olankitwanit, A.; Kathirvelu, V.; Rajca, S.; Eaton, G. R.; Eaton, S. S.; Rajca, A. *Chem. Commun.* **2011**, *47*, 6443–6445.

(36) Frisch, M. J. et al. *Gaussian 03, Revision E.01*; Gaussian: Wallingford, CT, 2004. Frisch, M. J. et al. , *Gaussian 09, Revision A.01*; Gaussian: Wallingford, CT, 2009.

(37) (a) Neese, F. *ORCA—an ab initio, density functional and semiempirical program package, Version 2.6*; University of Bonn: Bonn, 2008. (b) Allouche, A.-R. *J. Comput. Chem.* **2011**, *32*, 174–182.

(38) Rajca, A.; Mukherjee, S.; Pink, M.; Rajca, S. *J. Am. Chem. Soc.* **2006**, *128*, 13497–13507.

(39) Russell, G. A.; Chang, K. Y. *J. Am. Chem. Soc.* **1965**, *87*, 4381–4383.

(40) Two O-H···N hydrogen bonds are found between the two unique molecules of **3** (Figures S1 and S2, Supporting Information).

(41) Pedersen, C. J. *J. Am. Chem. Soc.* **1957**, *79*, 5014–5019.

(42) Hassal, C. H. The Baeyer−Villiger Oxidation of Aldehydes and Ketones. In *Organic Reactions*; Wiley: New York, 1957; Vol. 9, pp 73−106.

(43) Krow, G. R. The Baeyer−Villiger Oxidation of Ketones and Aldehydes. In *Organic Reactions*; Wiley: 1993; Vol. 43, pp 251−798.

(44) Demmin, T. R.; Rogic, M. M. *J. Org. Chem.* **1980**, *45*, 1153–1156.

(45) Oxidation of α-triketones with hydrogen peroxide in acetic acid provides dicarboxylic acids, which may be rationalized by the insertion of two oxygen atoms followed by hydrolysis and decarboxylation: Alder, K.; Reubke, R. *Chem. Ber.* **1958**, *91*, 1525–1535.

(46) Oxidation of 3,4-dihydro-2,2-dimethyl-2*H*-naphthol[1,2-*b*]pyran-5,6-dione with *m*-CPBA in DCM at room temperature provides cyclic anhydride and no products of epoxidation of the double bond: Yang, R.-Y.; Kizer, D.; Wu, H.; Volckova, E.; Miao, X.-S.; Ali, S. M.; Tandon, M.; Savage, R. E.; Chan, T. C. K.; Ashwell, M. A. *Bioorg. Med. Chem.* **2008**, *16*, 5635–5643.

(47) Oxidation of α,β-unsaturated ketones under the Baeyer−Villiger conditions may lead to mixtures of Baeyer−Villiger and epoxidation products.[43]

(48) Richmond, R. J.; Hassner, A. *J. Org. Chem.* **1968**, *33*, 2548–2551.

(49) Adam, J. M.; Winkler, T. *Helv. Chim. Acta* **1984**, *67*, 2186–2191.

(50) (a) As neither **8A** nor **8B** are isolated, computational determination of the kinetically-controlled regioselectivity between **8A** and **8B** would be prohibitive given the size and complexity of the present system and the expected small free energy differences between the relevant transition states. (b) Grein, F.; Chen, A. C.; Edwards, D.; Crudden, C. M. *J. Org. Chem.* **2006**, *71*, 861–872.

(51) Brady, K.; Hegarty, A. F. *J. Chem. Soc, Perkin Trans. 2* **1980**, 121–126.

(52) (a) Curtin, D. Y.; Miller, L. L. *Tetrahedron Lett.* **1965**, *23*, 1869–1876. (b) Curtin, D. Y.; Miller, L. L. *J. Am. Chem. Soc.* **1967**, *89*, 637–645.

(53) Removal of a phthaloyl protective group from acid and base sensitive compounds via an isoimide: (a) Kukolja, S.; Lammert, S. R. *J. Am. Chem. Soc.* **1975**, *97*, 5582–5583. (b) Crauste, C.; Froeyen, M.; Anné, J.; Herdewijn, P. *Eur. J. Org. Chem.* **2011**, 3437–3449.

(54) Wiitala, K. W.; Tian, Z.; Cramer, C. J.; Hoye, T. R. *J. Org. Chem.* **2008**, *73*, 3024–3031.

(55) Stockdill, J. L.; Behenna, D. C.; Stoltz, B. M. *Tetrahedron Lett.* **2009**, *50*, 3182–3184.

(56) Banerjee, A. K.; Mimo, M. S. L.; Vegas, W. J. V. *Russ. Chem. Rev.* **2001**, *70*, 971–990.

(57) Spagnol, G.; Rajca, A.; Rajca, S. *J. Org. Chem.* **2007**, *72*, 1867–1869.

(58) Photodecarbonylation, e.g., as reported for unsaturated or strained lactones, is considered to be less likely: (a) Chapman, O. L.; McIntosh, C. L. *J. Chem. Soc., Chem. Commun.* **1971**, 383–384. (b) Chapman, O. L.; Wojtkowski, P. W.; Adam, W.; Rodriguez, O.; Rucktaeschel, R. *J. Am. Chem. Soc.* **1972**, *94*, 1365–1367.

(59) The calculated NMR chemical shifts are for the lowest energy conformer of **4A** (Tables S5 and S6, Supporting Information).

(60) Tomasi, J.; Mennucci, B.; Cammi, R. *Chem. Rev.* **2005**, *105*, 2999–3094.

(61) Barone, G.; Gomez-Paloma, L.; Duca, D.; Silvestri, A.; Riccio, R.; Bifulco, G. *Chem.—Eur. J.* **2002**, *8*, 3233–3239.

(62) Nielsen, D. K.; Nielsen, L. L.; Jones, S. B.; Toll, L.; Asplund, M. C.; Castle, S. L. *J. Org. Chem.* **2009**, *74*, 1187–1199.

(63) 95−100% *m*-CPBA handled as solid is a potential hazard for detonation: (a) Heaney, H. *Top. Curr. Chem.* **1993**, *164*, 1–19. (b) *Technical Bulletin AL-116*, 1996, http://www.sigmaaldrich.com/etc/medialib/docs/Aldrich/Bulletin/al_techbull_al116.Par.0001.File.tmp/al_techbull_al116.pdf (accessed on Aug. 28, 2011).